Performance of Adaptive Beam Nulling in Multihop Ad Hoc networks under Jamming

Suman Bhunia, Vahid Behzadan, Paulo Alexandre Regis, Shamik Sengupta
Dept. of Computer Science and Engineering, University of Nevada, Reno, USA, 89557
sbunia@nevda.unr.edu, vbehzadan@unr.edu, pregis@nevada.unr.edu, ssengupta@unr.edu

***Abstract*—In a multihop ad hoc network, end-to-end data transmissions traverse through multiple inter-node wireless links. A jammer can disrupt the entire data transfer of a network by intentionally interfering with links between a subset of nodes. The impact of such attacks is escalated when the jammer is moving. While the majority of current ad hoc protocols consider omnidirectional transmission and reception, adaptive antennas can be utilized for spatial filtering of the jamming signal. This paper investigates the performance of employing adaptive beam nulling as a mitigation technique against jamming attacks in multihop ad hoc networks. Considering a moving jammer, the survivability of links and connectivity in such networks are studied by simulating various node distributions and different mobility patterns of the attacker. In addition, the impact of errors in estimation of direction of arrival and beamforming on the overall network performance are also examined. The results of this study indicate a significant improvement in retaining connectivity under jamming when adaptive beam nulling is applied.**

***Keywords*—Beamforming, Beam Nulling, multihop, Ad hoc, Anti-Jamming, Mobility.**

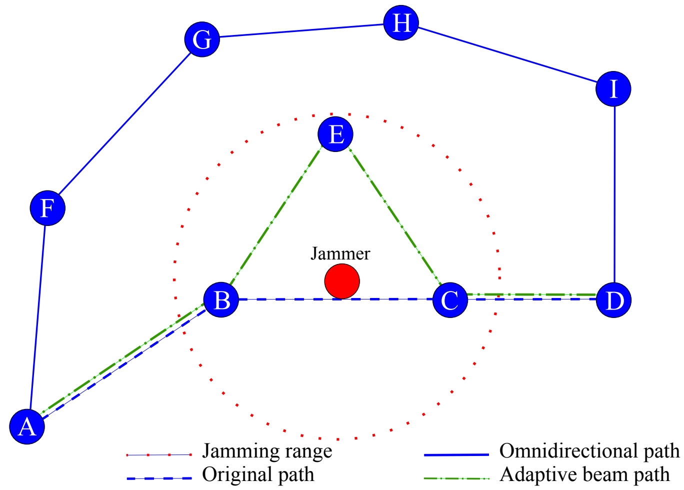

Fig. 1: A comparison of routing in omnidirectional vs beam nulling schemes under jamming

I. INTRODUCTION

The ecosystem of wireless communications is evolving towards independent, self-configuring architectures. Dependence of telecommunications on the infrastructure is envisioned to be largely diminished in a gradual move towards ad hoc networking. Especially, multihop ad hoc networks are predicted to play a key role in future mission critical communications, such as emergency radio networks in disaster zones, tactical mobile networks, and UAV communications. But the security of such networks heavily depend on the reliability of the wireless links. The open nature of wireless medium leaves the links inherently vulnerable to interference and jamming. In hostile environments such as battlefields, disrupting such links by means of jamming is an essential aim of an adversary's electronic warfare operations. Hence, mitigating jamming attacks has been a crucial research issue for the wireless community [1].

Some well-known categories of anti-jamming techniques proposed in the literature are those that utilize specially designed signal coding and modulation, such as Frequency Hopping Spread Spectrum (FHSS) [2] and Direct Sequence Spread Spectrum (DSSS) [3]. The downside associated with this class of techniques is their larger bandwidth requirement, which considering the state of the overcrowded electromagnetic spectrum, can prove to be costly. To preserve the scarce bandwidth, an alternative is to apply Spatial Filtering with beamforming antenna arrays [4]. This approach exploits the beamformers' ability to detect the Direction of Arrival (DoA) of signals. This direction is then used to modify the array's response so the interference sources are placed in the nulls of the antenna. Beamforming antenna systems that implement this mechanism are referred to as Adaptive Nulling Antennas (ANA).

The flow of information in multihop ad hoc networks can be disrupted by jamming a subset of nodes in a region. Traditionally, ad hoc configurations assume an omnidirectional antenna for communications. In multihop networks, data is routed over multiple hops to reach a destination that is not within communication range of the source. By adopting beam nulling techniques, a node can adapt its radiation pattern so a null is created in the direction of a jammer. This allows maintaining the links which are not affected by the jammer. Figure 1 provides an example of end-to-end data delivery in an ad hoc network. In the absence of a jammer, a packet follows through the path $A-B-C-D$ when all nodes employ omnidirectional antennas. In this configuration, the jammer can effectively jam nodes B, C and E. The routing protocol discovers the link failures and reroutes packets through $A-F-G-H-I-D$. This way packets are delivered but with an increased end-to-end delay and congestion on link $G-H$.

However, if nodes exploit beam nulling, nodes B, C and E can successfully avoid the jammer. Now packets can be delivered through $A-B-E-C-D$. Hence it can be seen that, in the presence of a jammer, adaptive beam nulling not only maintains the connectivity of the nodes inside the affected region, but also ensures less congestion on the remaining links.

The majority of the literature on ANAs rely on the assumption that the jammers are stationary with respect to beamformers (e.g. [5], [6], [7], [8], [9]), but with the recent expansion and growth of mobile wireless technologies, this assumption does not necessarily hold true. Also, there is a lack of publicly available analysis on the network performance of ad hoc networks utilizing adaptive nulling antennas under

This research was supported by NSF CAREER grant CNS #1346600

jamming. This paper aims to fill this gap by providing a network-oriented analysis via investigating the effects of a moving jammer on the connectivity and link survivability of an ad hoc network of nodes equipped with ANAs. For this purpose, multiple simulations have been performed to study the impact of jamming based on connectivity, number of islands, and number of surviving links for different node densities and jammer's mobility models. The simulation results show that the proposed mechanism can achieve up to 57.27% of improvement in connectivity over the omnidirectional antenna case.

The remainder of this paper is organized as follows: Section II provides a background on beam nulling techniques. The proposed methodology of adaptive beam nulling is presented in Section III. Section IV describes the simulation setup and results. Finally Section V concludes the paper.

II. Background

This section presents a discussion on terminology and concepts of adaptive nulling antennas. This is not intended to be a thorough overview of the beamforming and nulling techniques, but aims to provide the very basics to equip the reader with enough background to understand the rest of this paper. Interested readers are referred to [10] as a comprehensive source on beamforming and nulling antennas.

A. Antenna Terminology

Antennas are elements that couple electromagnetic energy between free space and a guiding structure [11]. Antennas may be classified based on how they radiate and receive energy in different directions. The directionality or gain of an antenna in a direction $d = (\theta, \phi)$ is defined as:

$$G(\vec{d}) = \eta \frac{U(\vec{d})}{U_{ave}} \tag{1}$$

Where η is the antenna efficiency, $U(\vec{d})$ is the power density in the direction of d, and U_{ave} is the average power density in all directions. An isotropic antenna is a radiator which has uniform gain in all directions ($U(\vec{d}) = U_{ave}$ for all directions). An omnidirectional antenna is defined as a radiator which has (relatively) constant gain in at least one 2-dimensional plane of directions. A directional antenna is one which radiates more energy in one or more directions compared to other directions. Antenna Radiation Pattern is the representation of the gain values in all or a subset of all directions. The pattern typically has a main lobe in which the gain is at its peak, and some side lobes. In this paper, we interchangeably refer to lobes as beams.

B. Adaptive Nulling Antennas

The circuitry of a beamforming antenna array is depicted in Figure 2. Signals coming from antenna elements consist of the desired signals, interference and noise. The control process determines individual weights of each signal based on an array response optimization method. In case of Adaptive Nulling Antenna (ANA) arrays, the weights are chosen so that the array response has nulls towards the directions of interference sources.

Various algorithms for adaptive estimation of Direction of Arrival (DoA) for both the desired and interference signals have been introduced and investigated in the literature. Such algorithms can be classified into beamscan algorithms and subspace algorithms [12]. Beamscan methods are based on scanning a conventional beam to cover a region and record the magnitude squared of the output. Examples of this class are Minimum Variance Distortionless Response (MVDR) and root MVDR [13]. On the other hand, Subspace algorithms exploit the orthogonality between the signal and noise subspaces. MUSIC, Root-MUSIC and ESPIRIT are among the most efficient subspace DoA estimation algorithms in antenna arrays [14]. A thorough review and comparison of widely used DoA estimation methods has been provided in [14].

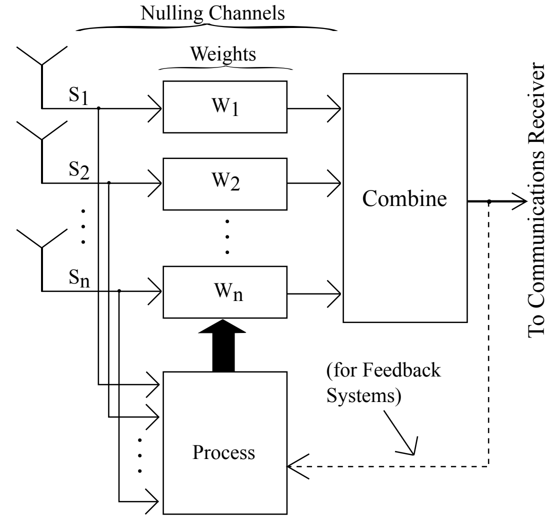

Fig. 2: Schema for ANA

Once the angular direction of an interference signal is determined, a beamformer calculates the weight values which result in a null towards the interference source. Some of the major weight calculation methods are Dolph-Chebyshev weighting, Least Mean Squares (LMS) and Conjugate Gradient Method (CGM) [15]. In the case of mobile ad hoc networks, in which the directions of desired and interference signals are not known and vary, Stochastic Search algorithms are applied [16]. Examples of such methods are Gradient Search Based Adaptive algorithms [17], [18], [19], Genetic Algorithms [20], [21], [22] and Simulated Annealing [23], [24]. Thorough reviews and comparison of beamforming methods and algorithms are provided in [16] and [25].

III. Methodology

A. Problem Statement

Figure 3 illustrates the effect of adaptive beam nulling in the presence of a moving jammer. In this scenario, the one hop links between node A and its neighbors B, C, D and E are considered. Node A periodically scans for the DoA of the jammer's signal (θ^m) in intervals of (τ) seconds. Due to the discontinuous observation of the jammer's DoA, while calculating the null angle, A must take into account the movement of the jammer between two consecutive observations. This calculation must include prediction of the jammer's angular velocity by considering its history of movements. As the mobility pattern of a jammer becomes more random, the prediction accuracy of its movements decreases. Therefore, the effect of various mobility patterns of the jammer on a network of beam nulling nodes can provide a practical measure for efficiency of this scheme.

Node A uses a modified beam pattern to communicate with its neighbors until the next sensing period. In Figure 3a,

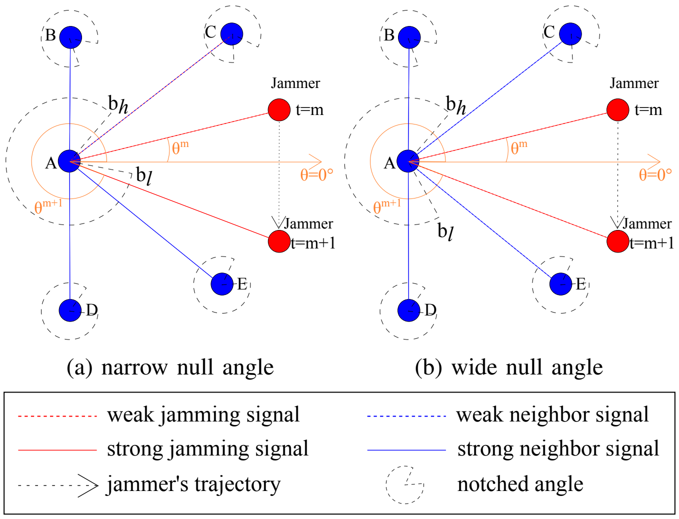

(a) narrow null angle (b) wide null angle

Fig. 3: Depiction of the beam nulling principle.

A has a narrower null angle compared to Figure 3b. With this narrow null angle, A can communicate with B, D and E, whereas with a wider null angle, A can communicate only with B and D. By the next sensing period the jammer moves to a new position, falling outside of the narrower null, which consequently exposes A to the jammer. As a result, all links are disrupted for A. On the other hand, the wider null angle maintains the jammer inside the null region for the whole interval. The trade-off for widening the null to cover the jammer's probable movements, is the cost of disabling unaffected links. Hence, another important factor in efficiency of beam nulling is the choice of optimum nulling angle in dynamic scenarios.

The practical limitations of adaptive beam nulling, such as inaccuracy in estimation of DoA, as well as hardware limitations in implementing a desired antenna pattern, lead to introduction of errors in a beamformer's performance. The aforementioned errors are formally defined as follows: the *measurement error* is the error in DoA estimation. If θ^c_{actual} is the actual angular position of the jammer with respect to A, but the observed value by A is $\theta^c_{observed}$, the measurement error is defined as $\theta^c_{actual} - \theta^c_{observed}$. Similarly, If a node calculates a null angle boundary at $b^c_{intended}$, but the implemented boundary is formed at $b^c_{implemented}$, *beamforming error* is defined as $b^c_{intended}$ - $b^c_{implemented}$. For a sensible study on the efficiency of a practical implementation, investigating the impact of inherent system errors in the simulation is of crucial importance.

B. System Assumptions

To investigate the effect and feasibility of adaptive beam nulling as a counter-measure for jamming attacks, a multihop wireless ad hoc network is considered. The nodes in this network are assumed to be static relative to each other. Each node is considered to be equipped with a beamforming antenna array, capable of introducing nulls in its originally omnidirectional radiation pattern. A node can not determine the DoA of jammer's signal while it is communicating with its neighbors. To determine the jammer's DoA it goes through a sensing phase at every τ seconds interval. If the received jamming signal is above an interference threshold it identifies an attack. The jammer is assumed to be a moving node with an omnidirectional antenna that continuously transmits a disrupting signal on the same frequency channel as the ad hoc network.

Even though the introduction of a null in an omnidirectional pattern of a beamforming node may be interpreted as changing the mode of communications to directional transmission, hence necessitating the use of Directional MAC protocols [26]. However, the higher network layers can continue to operate under the default assumption of omnidirectional transmission, since the nulled direction is already under jamming and no hidden/exposed terminal problem may arise from that direction [27].

C. Adaptive beam nulling

Let's consider a multihop ad hoc network of N nodes. After sensing the presence of a jammer, each node $i \in \mathbb{N}$ observes the angular position of the jammer or the angle of attack (θ^m_a) with its reference frame at every sensing phase $m \in \{1, ..., M\}$. Node i then adjusts its beamform to attenuate the signal from the jammer. i uses this beamform to communicate with its neighbors until the next sensing phase $(m+1)$. In Figure 3, at the m^{th} sensing phase, the jammer is sensed at angle θ^m_a. In the next sensing phase $(m+1)$, i senses the jammer at θ^{m+1}_a. Since the jammer is moving, it may cross the null of the beamform and i would be interfered by the jamming signal. The aim of adaptive beam nulling is to make sure the jammer stays within the nulled region for the entire time between sensing periods m and $m+1$. i calculates the angular velocity of the jammer as $(\theta^m_a - \theta^{m-1}_a)/\tau$, and keeps this value in a velocity array (v_a). Consider $\overline{v_a}$ and $\sigma(v_a)$ as the mean and standard deviation of the velocity (v_a), respectively.

Node i constructs a beam null using an algorithm that considers the history of jammer's movement. A beam null is defined by two boarders: b^m_l and b^m_h which are lower and higher angles respectively. Clearly, $\theta^m_a + \tau\overline{v_a}$ gives the estimated location of the jammer at the $(m+1)^{th}$ slot. Since the actual velocity and direction of the jammer are unknown, the null should be wider in case the jammer changes direction or velocity. Change of velocity of the jammer can be estimated with $\sigma(v_a)$. If a jammer changes its direction or velocity, $\sigma(v_a)$ would be high compared to the case when the jammer moves at the same direction with constant velocity. An estimation for the beam null angle can be calculated as:

$$b^m_h = \max(\theta^m_a,\ \theta^m_a + \tau(\overline{v_a} + \alpha\sigma(v_a))) \quad (2)$$

$$b^m_l = \min(\theta^m_a,\ \theta^m_a + \tau(\overline{v_a} - \alpha\sigma(v_a))) \quad (3)$$

$$\psi^m = b^m_l - b^m_l \quad (4)$$

Where ψ^m is the null angle constructed at the m^{th} sensing phase, and α is a multiplying factor. Note that the higher the value of α, higher the null angle is. Now, if the null is wider, chances are that more legitimate neighbors fall in this nulled region. A node i cannot communicate with its neighbor j if j is in the nulled region of i and vice versa. A higher value of α guarantees a higher probability that the jammer stays in the nulled region until the next sensing period. A very high value of α results in more deactivated links.

In Section IV-D1 we can observe that the system performance is a convex function w.r.t. α. Since the jammer's mobility pattern is not completely observable by a node, it should use adaptive value of α. To mitigate this effect, we propose a heuristic that dynamically adapts the value of α based on the observed history of jammer's movements.

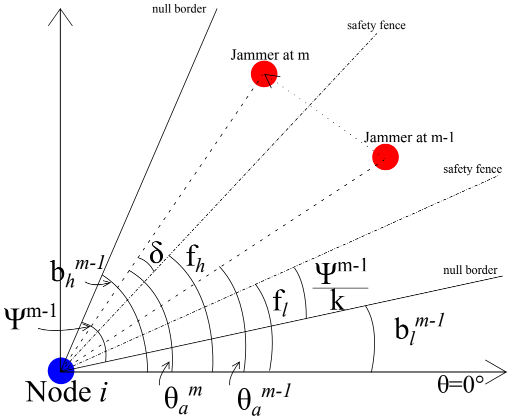

Fig. 4: Schema for adaptive α heuristics

D. *Heuristic for dynamic α*

Algorithm 1 presents a heuristic for adapting the value of α at each sensing period m. Figure 4 presents the schema for this adaptation. The beam null has been created in the previous sensing period $m-1$. At the m^{th} sensing slot, if the jammer stays inside the nulled region (ψ^{m-1}), then the node successfully avoids the attack. If the jammer is too close to the null border, α is increased. The algorithm considers a *safety zone* defined by two fences: f_h and f_l. We consider a factor $k \in (0, 0.5)$ which defines how defensive the network is. The safety fence is a ψ^{m-1}/k deviation from the null border towards the center of the null. Larger values of k lowers the probability of the jammer being in the safety zone, which consequently increases α, resulting in a wider null for the next interval. If the jammer stayed inside the safety zone, α is reduced by a factor of $\epsilon \in (0, 1)$. δ is calculated as the deviation of the jammer from the safety fence. At the m^{th} sensing phase, if the jammer is observed between the null border and the safety fence, α is increased by a factor of $(1 + \frac{k\delta}{\psi^{m-1}})$. This entails α is doubled if the jammer is at the null border. If the jammer crosses the null border, α is aggressively increased by a multiplying factor of $(1 + (\frac{k\delta}{\psi^{m-1}})^2)$.

IV. Simulation and Results

A. *Simulation setup*

A customized tick based simulator is developed to measure the performance of the proposed algorithm. Each tick represents the time interval (τ) between two consecutive sensing periods. The default parameters used are listed in Table I. Some parameters are varied to observe their effect on the performance. During the sensing phase, at each tick (m), every node checks for the jammer's angular position (θ_a^m). Each node then determines its new beamform according to eq. 4 and updates α using Algorithm 1. After the sensing and beamforming phases, communication with neighbors takes place until the time interval (τ) ends, when the same cycle is repeated.

Each simulation generates the position of each node randomly. The same set of positions are used to measure the performance of the network while varying other parameters. For simplicity, the simulator considers free space path loss model to calculate the received power. The simulator defines the links between two nodes on each iteration based on the received power from the corresponding neighbor and interference from the jammer at that moment. If the power received is above the cutoff and neither of the nodes are jammed, the simulator considers the link to be active.

Algorithm 1: Heuristics for dynamic α

```
ψ^{m-1} ← b_h^{m-1} − b_l^{m-1}
f_l ← b_l^{m-1} + ψ^{m-1}/k
f_h ← b_h^{m-1} − ψ^{m-1}/k
if f_l < θ_a^m < f_h then
    α ← εα
else if θ_a^m > b_l^{m-1} then
    δ ← θ_a^m − f_h
    α ← α(1 + (kδ/ψ^{m-1})^2)
end
else if θ_a^m < b_l^{m-1} then
    δ ← f_l − θ_a^m
    α ← α(1 + (kδ/ψ^{m-1})^2)
end
else
    if θ_a^m > f_h then
        δ ← θ_a^m − f_h
    else
        δ ← f_l − θ_a^m
    end
    α ← α(1 + kδ/ψ^{m-1})
end
```

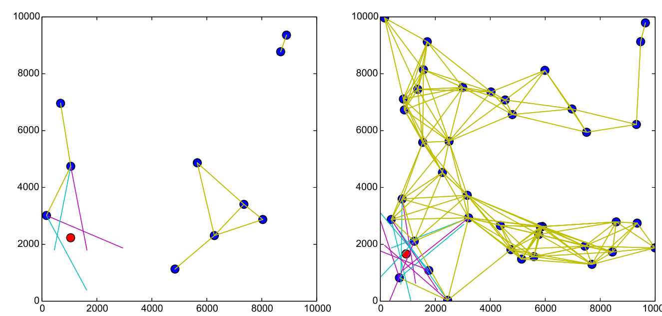

(a) simulation with 10 nodes (b) simulation with 100 nodes

Fig. 5: Snapshots of simulations

TABLE I: Simulation Parameters

Parameters	Symbol	Values
Simulation area		$10,000 \times 10,000\ m^2$
Transmission power	P_t	30 dBm
Received Power cutoff	P_r	-78 dBm
Communication Frequency		2.4 GHz
Communication Radious		3146 m
Initial α	α	
DOA error standard deviation	μ_{doa}	0.05
Beam nulling error standard deviation	μ_{bn}	0.05
Number of nodes simulated	N	100
Sensing interval	τ	50 ms
Simulation Time		500 s
Jammer mobility model		Random Walk

The simulator considers a scenario of N nodes scattered randomly in an area of $10,000 \times 10,000\ m^2$. Each node transmits with power of 30 dBm and the average communication radius is calculated as $3146m$. Figure 5a and Figure 5b depict snapshots of nodes during sensing intervals. One hop communication links are represented with yellow lines. The cyan and magenta lines represent the null borders b_l and b_h

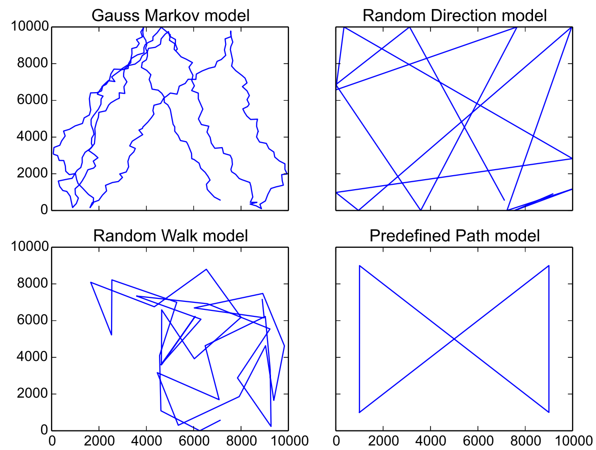

Fig. 6: Time domain sketch of different trajectory models

respectively. If the jammer is not in the proximity of a node to effectively jam it, the node does not use beam nulling. With effective beam nulling, the nodes keep some of their links active. In Figure 5a we can see 10 nodes present in the area. The network is not fully connected and there are 3 islands. Figure 5b shows a snapshot of simulation with 100 nodes. We can see that due to jamming, some links are deactivated but the network maintains its connectivity and no node is disconnected from the network.

The simulator considers the error in DoA estimation and beam nulling. A node observes DoA of the jammer as $\theta^c_{observed}$ while the actual DoA is θ^c_{actual}. For each node, the simulator generates $\theta^c_{observed}$ randomly based on a normal distribution with mean of θ^c_{actual} and standard deviation of μ_{doa}. Similarly the simulator introduces hardware limitation for beam nulling. If a node wants to form a beam null boundary at $b^c_{intended}$, the actual boundary is formed at $b^c_{implemented}$ which has a Gaussian distribution with mean of $b^c_{intended}$, and standard deviation μ_{bn}.

B. Jammer and mobility model

In this work a moving jammer is considered. Different mobility models of the jammer impact differently on a network. A mobility model defines how a node moves or changes its direction with time. The details of the selected models (Random Walk, Random Direction, Gauss-Markov, and a predefined path) can be seen in [28] and [29]. Random-based models are vastly used in the research community but they might not reproduce a realistic movement. Gauss-Markov is a temporal dependency model that can be considered more realistic, where the velocity and direction are correlated to the previous values, avoiding abrupt changes that occurs in the former models. A predefined path is also experimented assuming that a node follows a previously assigned path. Each model has its own influence in the performance of the network.

C. Performance Metrics

Three performance parameters are defined as follows:

- *Connectivity* is defined as the total number of connected pairs, which reflects how well connected a network is. It is defined as the summation of connected nodes. More precisely, connectivity of a network is $\frac{1}{2} \times (\sum_{i\in\mathbb{N}} \sum_{j\in\mathbb{N}} connected(i,j))$, where $connected(i,j) = 1$ if there exists at least one path from i to j and 0 otherwise.
- The second parameter is *average number of active links*. We consider a link as the one hop communication between two neighbors. A link may fail if either of the nodes is jammed or falls in the nulled region of the other one.
- The next performance parameter considered is the *average number of islands*. Some node may not be able to communicate with its neighbors. This results sometimes in a node being isolated from the rest of the network, or a group of nodes isolated from the other groups. We count the number of island present in the network periodically. If a network is completely connected, the number of island is 1. The higher amount of islands is, the more disrupted the network is.

The simulator monitors the above mentioned metrics at each iteration. It calculates the average of these matrices after the full simulation and record them as the result.

D. Results and Discussion

1) Discrete fixed α: In the initial phase of the simulation, the effect of α on system's performance is investigated. In this case the network is simulated without adaptive α, i.e. nodes do not use Algorithm 1. Figure Figure 7 presents the simulation results when α is fixed. The x-axis of these plots represent the discrete values of α that form the beam null in eq. 4. Nine different scenarios are considered: one benchmark scenario with no jamming and for each mobility model we simulated the network once with omnidirectional antenna, and once with the proposed beam nulling algorithm. The worst case scenario occurs when there is a jammer in the field and the nodes use omnidirectional antenna, consequently the performance is heavily affected by the presence of the jammer. The top benchmark result is obtained similarly to the worst case but with no jammer present, therefore the communications are not affected by any adversary. It can be seen from the results that when there is no jammer, the network is completely connected as the number of islands is 1. For a completely connected network with n nodes, the connectivity value is $\frac{n(n-1)}{2}$. Therefore, in a network of 100 nodes with no jammer, the connectivity is 4950, supporting the simulated result. When nodes do not use beam nulling islands are created, resulting in a poor connectivity value. Also it is observed that in the presence of a jammer, adaptive beam nulling significantly improves the overall performance in terms of all the metrics considered. In addition, when a jammer is present and the nodes do not apply beam nulling, the network is heavily affected, and a larger number of islands is created. However, when nodes apply adaptive beam nulling, different trajectory models perform differently with respect to the values of α.

It is noteworthy that for higher values of α, the number of average links may fall below the benchmark case of omnidirectional nodes in the presence of a jammer. This is because a higher value of α creates a wider null that results in deactivation of more links. A node may reduce this shortcoming by sensing the jammer more frequently but this also reduces the data communication window. In addition, it can be observed that as α increases, the average number of islands decreases, while the number of active links begin to deteriorate after a peak. This phenomenon can be interpreted

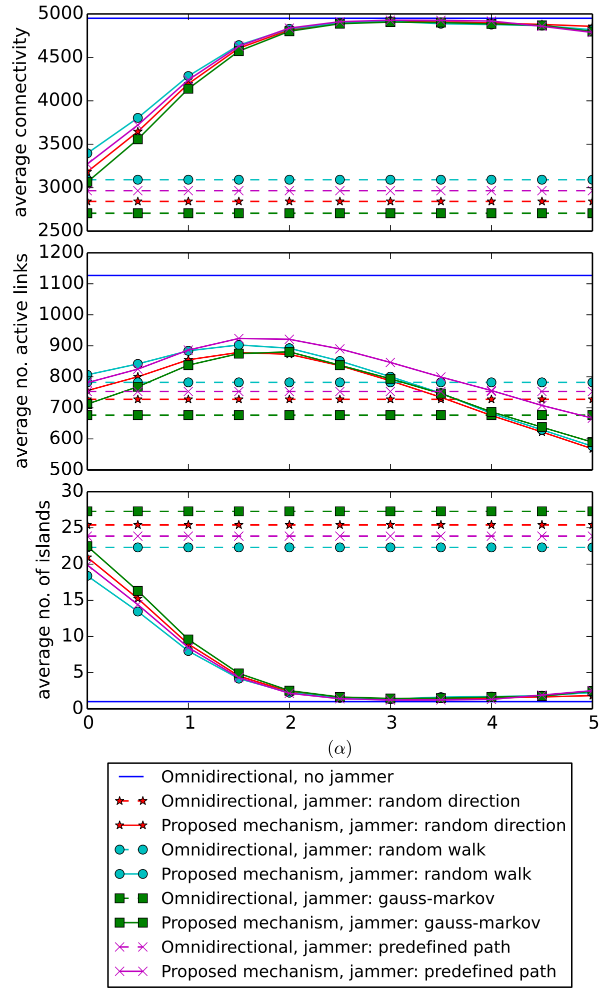

Fig. 7: Simulation results with fixed α

as a rise in congestion.

Another conclusion that can be derived from the results is that a fixed value of α does not guarantee the optimal performance, since the mobility pattern of the jammer is not known to any node. A node estimates the velocity of the jammer through periodic sensing. Therefore, the value of α must be dynamically updated based on the history of the jammer's movements.

2) Effect of Jammer's mobility model: Four different mobility models for the jammer are considered. Figure 8a illustrates the impact of these models on the defending network. It can be seen that the Random Direction and Random Walk models adversely affect the performances of the network, since the direction of the jammer undergoes abrupt changes in random intervals. For the predefined path and Gauss-Markov models, the direction and velocity are constant for the majority of the time, which allows adaptive beam nulling system to accurately estimate the jammer's movement. It is observed that for 100 nodes, the proposed mechanism achieves an improvement in connectivity of up to 57.27% relative to the omnidirectional under attack.

3) Effect of node density: Figure 8b illustrates the effect of varying number of nodes in the network which constitutes a change in the node density. It is observed that when a network is not well connected, the number of islands increases. As the number of nodes increases, connectivity is well preserved in the no jamming scenario. The jammer succeeds in disabling more links when the node density higher. Even though the number of link failures is on a similar level as the worst benchmark of omnidirectional with jamming, connectivity and number of islands demonstrate a better performance. In the benchmark scenario with omnidirectional antennas, the number of islands increases greatly with an increase in the number of nodes, since the density is higher and the attacker has more links in its jamming range. The proposed adaptive beam nulling approach succeeds in keeping the connectivity and number of islands close to the scenario of the benchmark with no jamming.

4) Effect of errors in beam nulling: As discussed earlier, errors are introduced in the simulator to account for the practical inaccuracies in beam nulling and DoA estimation. The effective beam null border is a random function with the mean of intended boarder angle and standard deviation of μ_{bn}. Similarly for each node the observed DoA is a random function of mean at the actual DoA and standard deviation of μ_{doa}. Figure 8c plots the performance of the network w.r.t. the error in the beam nulling. The X-axis is μ_{bn}, while the simulations are repeated with several different values of μ_{doa}. With a μ_{doa} of 0.1 that entails an error of 5.7^o in DoA measurement the connectivity still remains close to that of no jamming scenario. The plots reflect that both the error decreases the network performances significantly as the jammer is not tracked properly. However, with a higher value of error in measurement the proposed beam nulling mechanism still performs better than the omnidirectional antenna model.

V. Conclusion

This paper investigates the performance of adaptive beam nulling in multihop ad hoc networks under attack from a moving jammer. To illustrate the effectiveness of the proposed mechanism against jamming attacks, connectivity of various network topologies with different mobility patterns of the jammer are studied through simulations. Also, to increase the accuracy of the simulated models for practical implementations, effects of varying inherent errors on the performance of a beam nulling ad hoc network is considered. The results demonstrate a significant improvement in survivability of connectivity when adaptive nulling is used with our proposed mechanism.

References

[1] R. Saranyadevi, M. Shobana, and D. Prabakar, "Article: A survey on preventing jamming attacks in wireless communication," *International Journal of Computer Applications*, vol. 57, pp. 1–3, November 2012. Full text available.

[2] A. Yahya, O. Sidek, J. Mohamad-Saleh, and C. M. D. E. Center, "Performance analyses of fast frequency hopping spread spectrum and jamming systems.," *Int. Arab J. Inf. Technol.*, vol. 5, no. 2, pp. 115–119, 2008.

[3] L. B. Milstein, "Interference rejection techniques in spread spectrum communications," *Proceedings of the IEEE*, vol. 76, no. 6, pp. 657–671, 1988.

[4] B. D. Van Veen and K. M. Buckley, "Beamforming: A versatile approach to spatial filtering," *IEEE assp magazine*, vol. 5, no. 2, pp. 4–24, 1988.

[5] W. C. Cummings, "Anadaptive nulling antenna for military," *Lincoln Laboratory Journal*, vol. 5, no. 2, 1992.

[6] G. Okamoto, "Jammer nulling via low complexity blind beamforming algorithm," in *Antennas and Propagation Society International Symposium, 2007 IEEE*, pp. 25–28, IEEE, 2007.

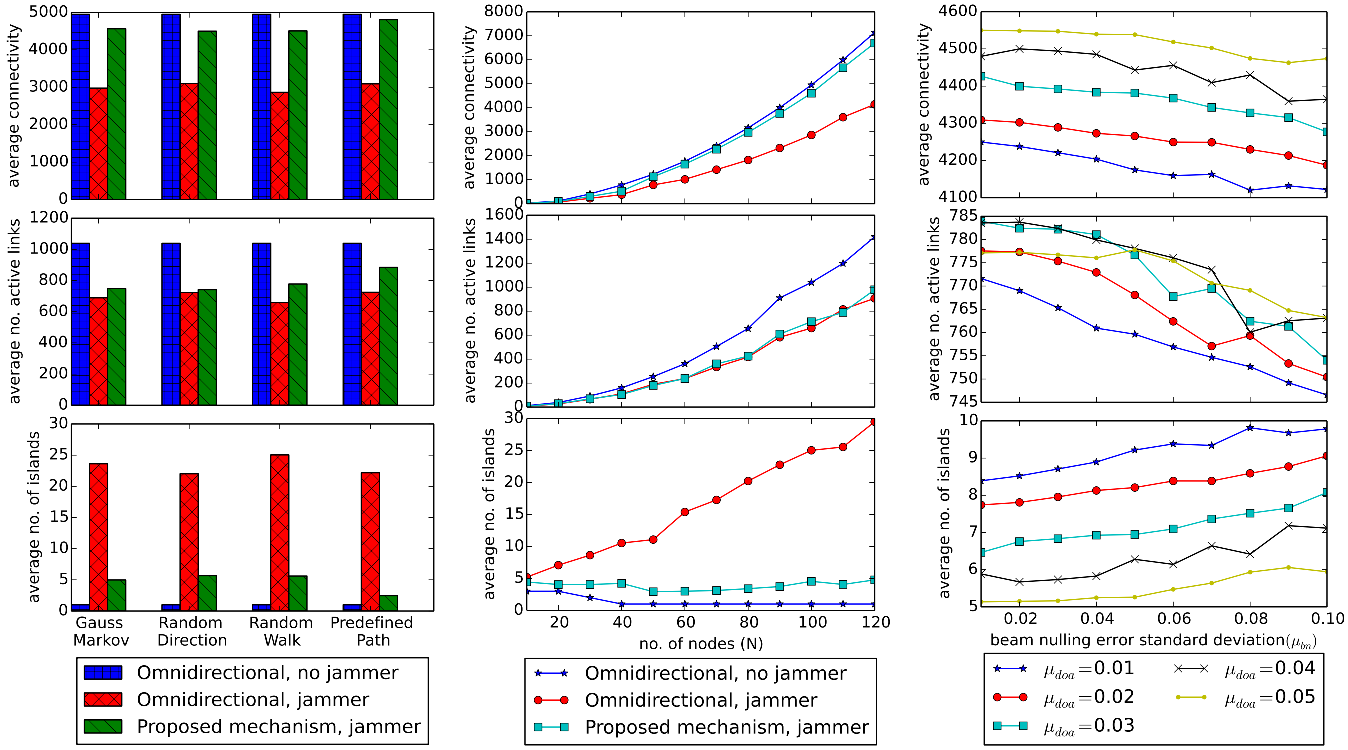

(a) different trajectory models

(b) varying number of Nodes

(c) varying error rate

Fig. 8: Simulation Results varying different simulation parameters

[7] W. Zhu, B. Daneshrad, J. Bhatia, H.-S. Kim, D. Liu, K. Mohammed, R. Prabhu, S. Sasi, and A. Shah, "Mimo systems for military communications," in *Military Communications Conference, 2006. MILCOM 2006. IEEE*, pp. 1–7, IEEE, 2006.

[8] D. Mingjie, P. Xinjian, Y. Fang, and L. Jianghong, "Research on the technology of adaptive nulling antenna used in anti-jam gps," in *Radar, 2001 CIE International Conference on, Proceedings*, pp. 1178–1181, IEEE, 2001.

[9] G. K. Rao and R. S. H. Rao, "Status study on sustainability of satellite communication systems under hostile jamming environment," in *India Conference (INDICON), 2011 Annual IEEE*, pp. 1–7, IEEE, 2011.

[10] J. C. Liberti and T. S. Rappaport, *Smart antennas for wireless communications: IS-95 and third generation CDMA applications*. Prentice Hall PTR, 1999.

[11] C. A. Balanis, *Antenna theory: analysis and design*. John Wiley & Sons, 2012.

[12] H. L. Van Trees, *Detection, estimation, and modulation theory*. John Wiley & Sons, 2004.

[13] C. Vaidyanathan and K. M. Buckley, "Performance analysis of the mvdr spatial spectrum estimator," *Signal Processing, IEEE Transactions on*, vol. 43, no. 6, pp. 1427–1437, 1995.

[14] V. Krishnaveni, T. Kesavamurthy, *et al.*, "Beamforming for direction-of-arrival (doa) estimation: A survey," *International Journal of Computer Applications*, vol. 61, no. 11, pp. 4–11, 2013.

[15] J. Volakis, *Antenna Engineering Handbook, Fourth Edition*. McGraw-Hill Companies,Incorporated, 2007.

[16] J. Becker, "Dynamic beamforming optimization for anti-jamming and hardware fault recovery," 2014.

[17] L. Lei, X. Rongqing, and L. Gaopeng, "Robust adaptive beamforming based on generalized sidelobe cancellation," in *Radar, 2006. CIE'06. International Conference on*, pp. 1–4, IEEE, 2006.

[18] Y. Xu and Z. Liu, "Noncircularity-rate maximization: a new approach to adaptive blind beamforming," in *Wireless Communications, Networking and Mobile Computing, 2009. WiCom'09. 5th International Conference on*, pp. 1–4, IEEE, 2009.

[19] S. Chen, L. Hanzo, N. N. Ahmad, and A. Wolfgang, "Adaptive minimum bit error rate beamforming assisted receiver for qpsk wireless communication," *Digital Signal Processing*, vol. 15, no. 6, pp. 545–567, 2005.

[20] R. Haupt and H. Southall, "Experimental adaptive nulling with a genetic algorithm," *MICROWAVE JOURNAL-EUROGLOBAL EDITION-*, vol. 42, pp. 78–89, 1999.

[21] A. Massa, M. Donelli, F. G. De Natale, S. Caorsi, and A. Lommi, "Planar antenna array control with genetic algorithms and adaptive array theory," *Antennas and Propagation, IEEE Transactions on*, vol. 52, no. 11, pp. 2919–2924, 2004.

[22] Y.-j. Lee, J.-W. Seo, J.-K. Ha, and D.-c. Park, "Null steering of linear phased array antenna using genetic algorithm," in *Microwave Conference, 2009. APMC 2009. Asia Pacific*, pp. 2726–2729, IEEE, 2009.

[23] D. J. Sadler, "Planar array design for low ambiguity," in *Antennas & Propagation Conference, 2009. LAPC 2009. Loughborough*, pp. 713–716, IEEE, 2009.

[24] H. Evans, P. Gale, B. Aljibouri, E. Lim, E. Korolkwiwicz, and A. Sambell, "Application of simulated annealing to design of serial feed sequentially rotated 2× 2 antenna array," *Electronics Letters*, vol. 36, no. 24, pp. 1987–1988, 2000.

[25] S. Ram, *A Study of Adaptive Beamforming Techniques Using Smart Antenna For Mobile Communication*. PhD thesis, National Institute of Technology Rourkela, 2007.

[26] O. Bazan and M. Jaseemuddin, "A survey on mac protocols for wireless adhoc networks with beamforming antennas," *Communications Surveys & Tutorials, IEEE*, vol. 14, no. 2, pp. 216–239, 2012.

[27] A. A. Ansari, Z. Hasan, M. J. Alam, K. Mohammad, and A. Siddique, "Performance comparison for omnidirectional and directional mac protocols for ad hoc network,"

[28] F. Bai and A. Helmy, "A survey of mobility models," *Wireless Adhoc Networks. University of Southern California, USA*, vol. 206, 2004.

[29] O. Bouachir, A. Abrassart, F. Garcia, and N. Larrieu, "A mobility model for uav ad hoc network," in *ICUAS 2014, International Conference on Unmanned Aircraft Systems*, pp. pp–383, 2014.